

Negative refraction, surface modes, and superlensing effect via homogenization near resonances for a finite array of split-ring resonators

M. Farhat,¹ S. Guenneau,² S. Enoch,¹ and A. B. Movchan²

¹*Institut Fresnel, CNRS, Aix-Marseille Université, Campus Universitaire de Saint-Jérôme, 13013 Marseille, France*

²*Department of Mathematical Sciences, University of Liverpool, Peach Street, Liverpool L69 3BX, United Kingdom*

(Received 10 March 2009; published 12 October 2009)

We present a theoretical and numerical analysis of liquid surface waves (LSWs) localized at the boundary of a phononic crystal consisting of split-ring resonators (SRRs). We first derive the homogenized parameters of the fluid-filled structure using a three-scale asymptotic expansion in the linearized Navier-Stokes equations. In the limit when the wavelength of the LSW is much larger than the typical heterogeneity size of the phononic crystal, we show that it behaves as an artificial fluid with an anisotropic effective shear modulus and a dispersive effective-mass density. We then analyze dispersion diagrams associated with LSW propagating within an infinite array of SRR, for which eigensolutions are sought in the form of Floquet-Bloch waves. The main emphasis is given to the study of localized modes within such a periodic fluid-filled structure and to the control of low-frequency stop bands associated with resonances of SRRs. Considering a macrocell, we are able to compute the dispersion of LSW supported by a semi-infinite phononic crystal of SRRs. We find that the dispersion of this evanescent mode nearly sits within the first stop band of the doubly periodic structure. We further discover that it is linked to the frequency at which the effective-mass density of the homogenized phononic crystal becomes negative. We demonstrate that this surface mode displays the hallmarks of all-angle negative refraction and it leads to a superlensing effect. Last, we note that our homogenization results for the velocity potential can be applied *mutatis mutandis* to designs of electromagnetic and acoustic superlenses for transverse electric waves propagating in arrays of infinite conducting SRRs and antiplane shear waves in arrays of cracks shaped as SRRs.

DOI: [10.1103/PhysRevE.80.046309](https://doi.org/10.1103/PhysRevE.80.046309)

PACS number(s): 47.65.-d, 47.35.Lf, 47.11.Fg, 47.11.St

I. INTRODUCTION

In 1968, Veselago [1] introduced the physical basis of negative refraction phenomenon (with optical index equal to -1), whereby light takes the wrong way i.e., the incident and the refracted wave vectors lie on the same side of the normal to the interface. Veselago further predicted the possibility of designing a flat convergent lens and numerous other unusual electromagnetic effects such as a reversed Cherenkov radiation and a reversed Doppler shift. Three decades afterward, Pendry [2] showed that a slab of left-handed material can be used to design a flat perfect lens that overcomes the Rayleigh limitation with a resolution less than $\lambda/2$ by taking into account the evanescent waves in addition to the radiative waves, thereby allowing the formation of a perfect image.

In 2000, Smith and Kroll [3] gave the experimental proof of negative index materials at gigahertz frequencies. Some scientific debates followed about causality and speed of light which should not be violated in spite of the negative refraction always present in a negative index material (see, e.g., [4,5]). The controversy was soon over and since then artificial structured metamaterials have raised growing interest and their design techniques have increased in sophistication leading to an extraordinary control of the permeability and permittivity gradients in order to construct complex lenses [6–13] and invisibility cloaks [14–19]. Photonic crystals (PCs) are the other alternatives to achieving such a negative refraction index. Metamaterials are in general based on repeated unit cells of conducting resonators (such as split-ring resonators); but unlike PCs, their periodicity is much smaller than the free space wavelength, allowing their homogeniza-

tion [20–27] from an electromagnetic point of view (we can characterize them by their effective electric permittivity and effective magnetic permeability). As for photonic crystals, all-angle negative refraction (AANR) takes place when the electromagnetic waves are modulated by the multiple Bragg scatterings leading to photonic stop bands where the directions of the group and phase velocities are opposite. In other words, the resonance of the wavelength of the incident field with the microstructure is responsible for negative refraction. Negative refraction has been demonstrated numerically and experimentally validated for liquid surface wave (LSW) [28–30] solutions of the linearized Navier-Stokes equations: LSW propagating within arrays of circular cylinders can also be focused. We have recently shown that such a liquid lensing effect was possible for square arrays of close-to-touching square cylinders. In that case, the array can be approximated by a lattice of thin water channels [31], for which dispersion curves are given in closed form and thus the frequency of AANR. Broadband cloaking of LSW via homogenization of a periodic array of cylinders has been recently demonstrated both numerically and experimentally [32].

In this paper, we focus on the use of split-ring resonator (SRR) structures [33–35] in the domain of linear liquid surface waves. We first derive the governing equations of LSW propagating within a square array of fixed cylinders from the linearized Navier-Stokes equations, then we present an analysis of dispersion curves of a single SRR in a unit cell: we set the spectral problem for the Helmholtz operator within a doubly periodic square array of SRR, homogeneous Neumann boundary conditions are prescribed on the contour of each resonator, and the standard Floquet-Bloch conditions

are set on the boundary of an elementary cell of the periodic structure, which presents a LSW band gap at low frequencies. We show through asymptotic analysis of our thin-walled periodic structure that we can estimate accurately the frequency of the first localized mode and henceforth the frequency of the first band gap.

The aim of our work is to demonstrate the existence of evanescent waves [36] propagating at the interface separating the phononic crystal from the surrounding liquid with frequencies restrained to the first LSW band gap. To do so, we use the supercell method [37,38], which consists here of a truncated crystal surrounded by perfectly matched layers (PMLs) in one direction, with Floquet-Bloch conditions in the other. This enables us to find the modes supposed to propagate in the crystal and among them the surface modes we are looking for (evanescent in the surrounding liquid). We then compute the dispersion curve of the first surface mode, which compares well with its asymptotic estimate. Finally, we show that negative refraction occurs at a frequency located nearly within the first gap and that the resolution of the image is about $\lambda/3$, with λ as the wavelength of the source.

II. HOMOGENIZATION OF AN ARRAY OF SRR NEAR RESONANCE

This section is concerned with the homogenization of a periodic structure involving resonant elements. The resonances are associated with fast-oscillating field in thin bridges, and we filter these oscillations by introducing a third scale in the usual two-scale expansion. To keep things simple, we start with the Helmholtz equation (obtained from linearizing the Navier-Stokes equation in the context of surface liquid waves, see the next section, but also valid in some electromagnetic or acoustic settings) and we consider an open bounded region $\Omega_f \subset \mathbb{R}^2$. This region is, e.g., a fluid-periodic structure consisting of a square array of (the cross section of) split-ring resonators shaped as the letter C,

$$\nabla^2 \phi_\eta + \kappa^2 \phi_\eta = 0, \quad \text{in } \Omega_f \setminus \overline{\Theta}_\eta, \quad \frac{\partial \phi_\eta}{\partial n} = 0, \quad \text{on } \partial \Theta_\eta, \quad (1)$$

where $\Theta_\eta = \cup_{i \in \mathbb{Z}^2} \{\eta(i+C)\}$ with η as a small positive parameter, that is, $0 < \eta \ll 1$. Moreover, $\frac{\partial}{\partial n}$ stands for $\mathbf{n} \cdot \nabla$ with \mathbf{n} as the outward unit normal to $\partial \Theta_\eta$. Note also that the number of SRRs in the phononic crystal Ω_f is an integer that scales as η^{-2} . Formally, a split ring C can be modeled as

$$C = \{a < \sqrt{x_1^2 + x_2^2} < b\} \setminus \overline{\Pi}_\eta, \quad (2)$$

where a and b are functions of variables x_1, x_2 unless the ring is circular and

$$\Pi_\eta = \{(x_1, x_2): 0 < x_1 < l, |x_2| < \eta h/2\} \quad (3)$$

is a thin ligament of thickness ηh and length $l = b - a$ between the ends of the letter C.

Our aim is to show that the homogenized multistructured fluid-periodic structure within Ω_f is characterized by an effective density which can take negative values near the fun-

damental resonance of the SRR. For this, we note that when the fluid penetrates the multiply connected region $\Omega_f \setminus \overline{\Theta}_\eta$, it undergoes fast periodic oscillations when moving from one cell $\eta Y = [0, \eta]^2$ to the adjacent ones, in both x_1 and x_2 directions. To filter these oscillations, we consider an asymptotic expansion of the potential field solution of the Helmholtz equation (1) in terms of a macroscopic (or slow) variable $\mathbf{x} = (x_1, x_2)$ and a microscopic (or fast) variable \mathbf{x}/η . Moreover, the fluid undergoes faster oscillations in the x_2 direction when it penetrates the thin cut of each SRR C, so that the asymptotic expansion of the potential should be sought in the form

$$\forall \mathbf{x} \in \Omega_f, \quad \phi_\eta(\mathbf{x}) = \phi_0\left(\mathbf{x}, \frac{\mathbf{x}}{\eta}, \frac{x_2}{\eta^2}\right) + \eta \phi_1\left(\mathbf{x}, \frac{\mathbf{x}}{\eta}, \frac{x_2}{\eta^2}\right) + \eta^2 \phi_2\left(\mathbf{x}, \frac{\mathbf{x}}{\eta}, \frac{x_2}{\eta^2}\right) + \dots, \quad (4)$$

where $\phi_i: \Omega_f \times Y \times [-h/2, h/2] \rightarrow \mathbb{C}$ is a smooth function of variables $(\mathbf{x}, \mathbf{y}, \xi) = (x_1, x_2, y_1, y_2, \xi)$, independent of η , such that $\forall \mathbf{x} \in \Omega_f$, $\phi_i(\mathbf{x}, \cdot, \xi)$ is Y periodic, and h denotes the thickness of the thin cut of the SRR C.

The differential operator is rescaled accordingly as $\nabla = \nabla_{\mathbf{x}} + (1/\eta)\nabla_{\mathbf{y}} + (1/\eta^2)\nabla_{\xi}$, so that Eq. (1) can be re-expressed as

$$\left\{ \left(\nabla_{\mathbf{x}} + \frac{1}{\eta} \nabla_{\mathbf{y}} + \frac{1}{\eta^2} \nabla_{\xi} \right) \cdot \left(\nabla_{\mathbf{x}} + \frac{1}{\eta} \nabla_{\mathbf{y}} + \frac{1}{\eta^2} \nabla_{\xi} \right) + \kappa^2 \right\} \times \left\{ \sum_{i=0}^{\infty} \eta^i \phi_i\left(\mathbf{x}, \frac{\mathbf{x}}{\eta}, \frac{x_2}{\eta^2}\right) \right\} = 0, \quad (5)$$

with the notations $\nabla_{\mathbf{x}} = (\partial/\partial x_1, \partial/\partial x_2)$, $\nabla_{\mathbf{y}} = (\partial/\partial y_1, \partial/\partial y_2)$, and $\nabla_{\xi} = (0, \partial/\partial \xi)$. Collecting terms of the same power of η in Eq. (5), we obtain the following homogenized problem in the limit when η tends to zero, in the phononic crystal Ω_f :

$$(\mathcal{P}_{hom}): \nabla \cdot \{ [\mu_{hom}] \nabla [\rho_{hom}^{-1} \phi_{hom}(\mathbf{x})] \} = \kappa^2 \phi_{hom}(\mathbf{x}), \quad (6)$$

with the effective shear modulus (sometimes called shear viscosity in the literature on anisotropic fluids even if it is related to strain, whereas viscosity rather goes with velocity gradient or strain rate) is given by

$$[\mu_{hom}] = \frac{1}{\text{area}(Y^*)} \begin{pmatrix} \text{area}(Y^*) - \psi_{11} & \psi_{12} \\ \psi_{21} & \text{area}(Y^*) - \psi_{22} \end{pmatrix},$$

where $Y^* = Y \setminus \overline{C}$ and ϕ_{ij} represent corrective terms defined by

$$\forall i, j \in \{1, 2\}, \quad \psi_{ij} = - \int_{\partial C} \Psi_j n_i ds, \quad (7)$$

where $\mathbf{n} = (n_1, n_2)$ is the unit outward normal to C and Ψ_j are periodic potentials which are unique solutions (up to an additive constant) of the following annex problems (\mathcal{K}_j):

$$(\mathcal{K}_j): \nabla^2 \Psi_j = 0 \quad \text{in } Y^*, \quad \frac{\partial \Psi_j}{\partial n} = -\mathbf{n} \cdot \mathbf{e}_j, \quad \text{on } \partial C, \quad (8)$$

with $(\mathbf{e}_1, \mathbf{e}_2)$ as the canonical basis in \mathbb{R}^2 .

From Eq. (6) (where derivatives are understood in a weak sense, i.e., they include discontinuities), we deduce that the

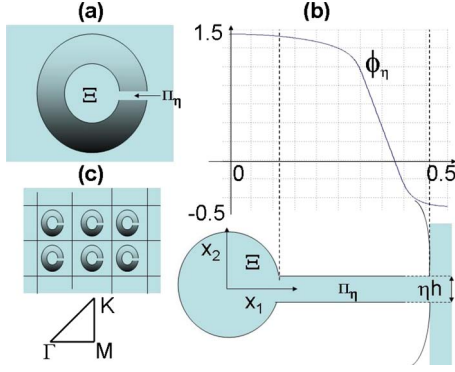


FIG. 1. (Color online) (a) Geometry of the problem in a basic cell; (b) corresponding one-dimensional (1D) profile of the velocity potential along the x_1 direction at the frequency $\kappa=1.95$ (we note that ϕ_η is almost constant in Ξ , whereas it varies rapidly in the thin-bridge Π_η); (c) periodic array of SRR and associated reduced Brillouin zone ΓMK in the reciprocal space.

effective transmission conditions at the boundary of the phononic crystal $\Omega_f \setminus \Theta_\eta$ are

$$\phi_{hom}^{(i)}|_{\partial\Omega_f^-} = \text{area}(Y^*) \phi_{hom}^{(e)}|_{\partial\Omega_f^+} \quad (9)$$

for the homogenized potential and

$$n \cdot ([\mu_{hom}] \nabla \phi_{hom}^{(i)})|_{\partial\Omega_f^-} = n \cdot (\nabla \phi_{hom}^{(e)})|_{\partial\Omega_f^+} \quad (10)$$

for its normal derivative.

The effective density ρ_{hom} is given in the form

$$\rho_{hom}(\kappa) = 1 - \sum_{m=1}^{\infty} \frac{\kappa^2}{\kappa^2 - \kappa_m^2} \|V_m\|_{L^2(0,l)}^2, \quad (11)$$

where the eigensolutions V_m correspond to longitudinal vibrations of the liquid-filled thin cut Π_η within the split-ring resonator. The Zhikov function (11) also appears in the homogenization of high-contrast media [39–43]. In the context of electromagnetism, it was first introduced by O’Brien and Pendry to design high-contrast photonic crystals displaying artificial magnetism [44].

It is clear from Eq. (11) that $\rho_{hom}(\kappa)$ takes negative values near resonances $\kappa = \kappa_m$. For our purpose, it is enough to look at the first few resonant frequencies κ_m (the higher the frequency the worse the asymptotic approximation). These frequencies are associated with vibrations V_m of the thin domain Π_η [34] as follows:

$$V_m''(x_1) + \kappa_m^2 V_m(x_1) = 0, \quad 0 < x_1 < l, \quad (12)$$

$$V_m(0) = 0, \quad (13)$$

$$\eta h V_m'(l) = \text{area}(\Xi) \kappa_m^2 V_m(l), \quad (14)$$

where ηh and l are, respectively, the thickness and the length of the thin ligament Π_η and Ξ is the central disk within the SRR [see Fig. 1(a)]. The ligament Π_η is connected to Ξ ; hence, $V(l) = V$, where V is the vibration of the water cavity Ξ . Note that the derivation of Eq. (14) required a boundary layer analysis, and we refer to [45–47] for more details.

The solution of the problem (12)–(14) has the form

$$V_m(x_1) = A \sin(\kappa_m x_1), \quad (15)$$

where κ_m satisfies the following transcendental equation:

$$\eta h \cot(\kappa_m l) = \text{area}(\Xi) \kappa_m. \quad (16)$$

The above three-scale analysis holds for the cases of transverse electric waves propagating within an array of infinitely conducting cylindrical fibers whose cross section is a SRR. In this case, our analysis shows the mechanism leading to artificial magnetism (in which case $[\mu_{hom}]$ should be replaced with the inverse homogenized permittivity matrix $[\epsilon_{hom}]^{-1}$ and ρ_{hom} should be replaced with the scalar homogenized permeability μ_{hom}). It also holds for the case of anti-plane shear waves propagating within an isotropic elastic material with cracks shaped as SRR. In the sequel, we focus our analysis on the liquid surface wave problem. To start with, we give a brief outline of the derivation of the Helmholtz equation for LSW.

III. GOVERNING EQUATIONS FOR LIQUID SURFACE WATER WAVES

A. Setup of the problem on a free surface

Let Ω denotes the region of the vessel in \mathbb{R}^3 occupied by the fluid. For our study, we choose a specific liquid [48] with a low viscosity constant to avoid the appearance of boundary layers which prevent the propagation of the liquid between the cylinders.

We further assume that the propagation speed of vibrations at the surface of the liquid is much smaller than their sound speed in the fluid, i.e., we consider that our liquid is incompressible (divergence free). This means that the pressure field of the liquid depends only on phenomena occurring at the air-liquid interface (no dilatation effects). Assuming that the fluid is also irrotational, we know that there exists a velocity potential Φ such that

$$\nabla^2 \Phi = 0 \quad \text{in } \Omega. \quad (17)$$

This Laplace equation does not manifest a wave character: waves are induced by the boundary conditions on the free surface $x_3 = s(x_1, x_2, t)$ separating the liquid and air, where x_3 is the vertical coordinate that is perpendicular to the horizontal plane (x_1, x_2) . The plane $x_3 = 0$ corresponds to the bottom of the water tank.

Assuming that liquid fluctuations are small around the mean value $x_3 = p$ (liquid depth), differentiation with respect to the time variable t in the linearized Navier-Stokes equations leads to the Poisson condition [49]

$$\frac{\partial^2 \Phi}{\partial t^2} + g \frac{\partial \Phi}{\partial x_3} - \frac{\sigma}{\rho} \frac{\partial \nabla^2 \Phi}{\partial x_3} = 0 \quad \text{on } x_3 = p, \quad (18)$$

where g is the acceleration caused by gravity and σ is the surface tension (e.g., due to capillarity effects).

The boundary value problem (17) and (18) is completely specified provided that the normal derivative of Φ vanishes at the bottom of the vessel (Neumann or “no-flow” boundary condition), bringing

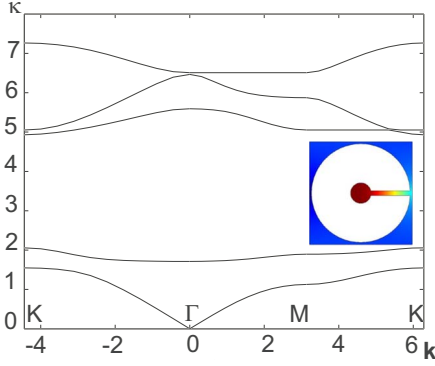


FIG. 2. (Color online) Band diagram for a doubly periodic square lattice of SRR representing the spectral parameter κ versus the Bloch vector \mathbf{k} in the first Brillouin zone ΓMK ; inset: map of the eigenmode corresponding to $\kappa_1 = 1.547$ in a unit cell with a SRR of outer radius $0.48d$ and inner radius $0.1d$ and thickness of the thin ligament Π_η equal to $\eta/h = 0.05d$, with $d = 1$ as the pitch of the array.

$$\mathbf{n} \cdot \nabla \Phi = 0 \quad \text{on } x_3 = 0. \quad (19)$$

B. Dispersion relation linking the spectral parameter κ to the wave frequency ω

Let us now consider a water tank filled with an array of fixed rigid cylinders in the form of SRR attached to the bottom. We look for harmonic liquid surface waves characterized by their velocity potential Φ as follows:

$$\Phi(x_1, x_2, x_3, t) = \text{Re}[\phi(x_1, x_2) \cosh(\kappa x_3) e^{-i\omega t}], \quad (20)$$

where ω denotes the wave frequency and κ is a spectral parameter related to the reduced potential ϕ through the Helmholtz equation

$$(\nabla^2 + \kappa^2)\phi = 0. \quad (21)$$

The spectral parameter in Eq. (21) is linked to the wave frequency through the dispersion relation

$$\omega^2 = g\kappa(1 + l_c^2 \kappa^2) \tanh(\kappa p), \quad (22)$$

where $l_c = \sqrt{\sigma/(\rho g)}$ is the liquid capillarity length related to the surface tension in Eq. (18), p is the liquid depth, and g is the gravity acceleration.

C. Spectral problem for Floquet-Bloch water waves

It remains to model the doubly periodic array of SRRs, as in Fig. 2. These are embedded within an elementary cell $Y = [0, 1] \times [0, 1]$ repeated periodically in the plane $(x_1 - x_2)$. Our spectral problem is thus completely specified if we finally assume that the normal derivative $\frac{\partial \phi}{\partial n}$ of the reduced potential ϕ vanishes on each rigid cylinder (Neumann or no-flow boundary condition) and the reduced potential also fulfills the Floquet-Bloch condition

$$\phi(x_1 + 1, x_2 + 1) = \phi(x_1, x_2) e^{i(k_1 + k_2)}, \quad (23)$$

with the Bloch vector $\mathbf{k} = (k_1, k_2) \in Y^* = [0, \pi]^2$, where Y^* is the first Brillouin zone.

It is interesting to note that LSW obeys the same Helmholtz equation (21) and limit conditions (Neumann and Floquet-Bloch) as would electromagnetic waves (H_\parallel) propagating in a homogeneous isotropic dielectric medium (take $\kappa = \omega^2 n^2$, with n as the refractive index of, say, silica) containing a periodic assembly of infinite conducting inclusions. The mathematical model also holds for antiplane shear waves propagating within an isotropic elastic material with cracks (take $\kappa^2 = \omega^2 \rho / \mu$ with μ and ρ as the shear modulus and the density of, say, silica, with Neumann data standing for traction free boundary conditions). Nevertheless, the propagation of LSW is further constrained by the dispersion relation (22): LSWs are always dispersive (even in a homogeneous liquid), unlike their electromagnetic and elastic counterparts.

The characterization of the dispersive properties of LSW in fluid-periodic structures is the goal of the next section. For this, we analyze the band diagrams of an infinite array of SRRs and then demonstrate the existence of surface modes at the surface of the crystal by truncating the crystal in one direction of space (which is then modeled using perfectly matched layers), while we set Floquet-Bloch conditions in the other direction. Finally, we show that negative refraction can be achieved with this phononic crystal and that the resolution of the image we obtain is subwavelength.

IV. ANALYSIS OF BAND DIAGRAMS

To investigate numerically the stop-band properties for out-of-plane LSW propagating within the array of SRRs, we use the finite element method (by implementing the weak form of Eq. (21) in the commercial software COMSOL); see, e.g., [50] for more details on enforced Floquet-Bloch conditions. In Fig. 2, we give the band diagram for normalized eigenfrequencies κ as a function of the projection of the Bloch vector \mathbf{k} on the first Brillouin zone ΓMK . We consider a square array of normalized pitch $d = 1$ (take $d = 1$ cm for comparisons with [31]) with embedded SRR of inner radius $0.1d$ and outer radius $0.48d$ with a thin cut (ligament) of thickness $0.05d$.

Figure 2 displays two full phononic band gaps for the range of spectral parameters $\kappa \in [1.546, 2.056]$ and $\kappa \in [2.056, 4.93]$. As depicted in a previous study [34], the low-frequency band gap (the first one) is associated with the resonant modes of a single SRR (microscopic structure), while the second one is due to some Bragg scattering phenomenon (macroscopic structure). We also plot in Fig. 2 the corresponding localized eigenfunction (the first eigenmode) which corresponds, in the context of continuum mechanics, to oscillations of the central region of the SRR as a rigid solid connected to the fixed rigid region around it via the thin cut Π_η (acting like a spring) [34,46]. In our context of LSW, this can be interpreted as some collective motion of water particles moving together up and down in each SRR.

The transcendental equation (16) can be further simplified if we look at the first low frequency, for which we deduce the explicit asymptotic approximation

$$\kappa_1 \sim \sqrt{\frac{\eta h}{\text{area}(\Xi) l}}. \quad (24)$$

Our numerical estimate is

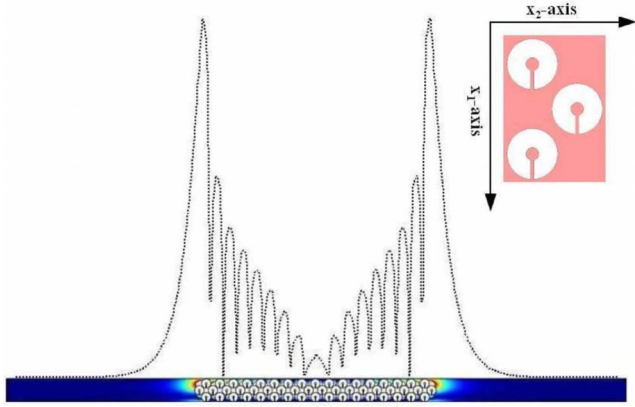


FIG. 3. (Color online) 2D field map of the surface mode at the frequency $\kappa=1.95$ and the corresponding 1D profile along the x_2 direction; inset: a row in the truncated crystal.

$$\kappa_1 \sim \sqrt{\frac{0.05}{0.38}} \sqrt{\frac{1}{\pi 0.1^2}} = 2.047, \quad (25)$$

which is in excellent agreement with the finite element value for the plasmon frequency $\kappa=2.056$ occurring at the K point when $\mathbf{k}=(\pi, \pi)$.

We note that, at the plasmon frequency, the vibration of the thin ligaments is enhanced, which is in accordance with the behavior of the field as observed in Fig. 5. It is therefore important to incorporate the resonances within the thin bridges, as we did, to model the frequency at which negative refraction occurs.

A. LSW surface modes: Physical discussion and numerics

In this section, we show that phononic crystals support LSW surface modes. These waves are exponentially localized at the interface between the liquid and either side of the phononic crystal.

Unlike for the case of metal-dielectric interfaces where the localization of surface waves results from the negative dielectric constant in the metal for a range of frequencies, LSW Bloch waves are here localized thanks to interference effects in the phononic crystal. These surface states can be classified in four types [38] corresponding to their behavior, i.e., extended or decaying, both in the liquid and in the crystal. Our study corresponds to LSW exponentially localized at the interface: the wave is decaying both in the homogeneous region occupied by the liquid and in the crystal, as can be seen in Fig. 3.

As outlined by Pendry, surface modes are vital in the process of focusing a point source with a photonic crystal in order to achieve a perfect lens by overcoming the Rayleigh limitation [2]. To the best of our knowledge, the investigation of these modes for LSW has never been made; the nearest study we came across is on effective medium theory applied to surface plasmons in structured interfaces [51]. That is the reason why, in this section, we will demonstrate the existence of such modes at the interfaces of a phononic crystal consisting of SRR as described previously.

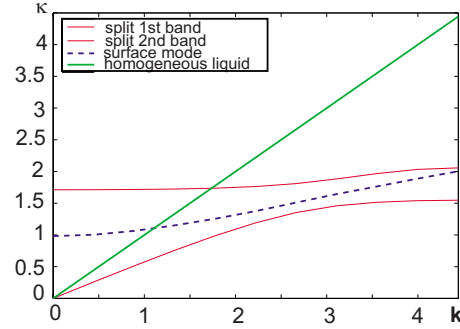


FIG. 4. (Color online) Band diagram of surface mode in Fig. 3. The red (gray) acoustic and optical curves represent the first two bands of the diagram of a single SRR in the ΓM direction (see Fig. 2); the dashed curve represents the dispersion of the surface mode and in green (light gray) we show the straight “sound line.”

In order to study these modes, we employ the supercell method in which slabs of the PC alternate with liquid regions: we use 17 periodic cells of PC (see the inset in Fig. 3) and six cells of homogeneous liquid on either side of the truncated PC (see Fig. 3). Floquet-Bloch conditions are applied in the x_1 direction (see top and bottom walls in Fig. 3) since the crystal is supposed to be infinite in this direction. However, in the x_2 direction the crystal is of finite size (consisting of 35 rows of SRR); hence, we consider a surrounding homogeneous liquid of same area as the crystal in order to catch the decay of the surface modes. Because the surface states are strongly localized to the uppermost PC layer, the error introduced by the finite size of the slab could well be negligible, but we added a PML region at the end of each homogeneous liquid region (i.e., at the leftmost and rightmost boundaries of the supercell shown in Fig. 3) to further improve the accuracy of the numerical model.

We use the finite element method (implemented in COMSOL) to find the eigenvalues of the supercell previously described and the corresponding modes which are both decaying and propagating. We can see in Fig. 3 the two-dimensional (2D) field map corresponding to the surface mode with a frequency $\kappa=1.95$, which as expected, has a frequency in the first band gap. This mode is decaying both in the homogeneous liquid and in the crystal and is thus exponentially localized at the upper and lower interfaces.

Let us now focus on the band structure of the interface of the crystal. In Fig. 4, we plot the dispersion curve of the surface mode shown in Fig. 3 by varying the Bloch vector in the ΓM zone and by calculating the corresponding eigenfrequencies. We plot in the same figure, the ΓM portion of Fig. 2 and the “light line” corresponding to a wave propagating in the homogeneous liquid.

As previously noticed, the width of the first band gap is much smaller than the width of the second one, and this explains why it is more difficult to find numerically its surface modes. The region of interest for our study is for $|\mathbf{k}_{Bloch}| > \kappa$. More precisely the mode is localized near the M point of the Brillouin zone and its frequency κ is equal to 1.95. Because LSW cannot propagate within the band gap, we can deduce that this mode is an evanescent one.

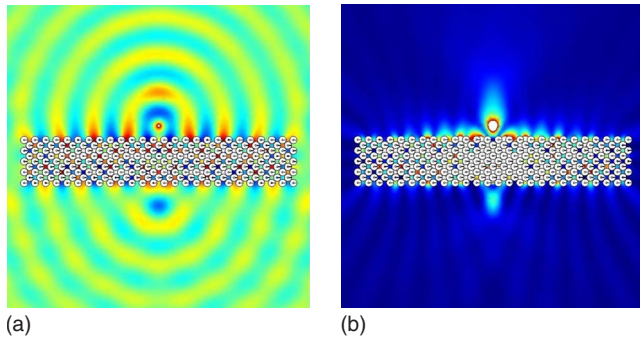


FIG. 5. (Color online) LSW patterns [potential ϕ for (a) and its square modulus $|\phi|^2$ for (b)] for one point source at a frequency lying near the lower edge of the second band ($\kappa=1.95$ i.e., close to the asymptotic estimate $\kappa_1 \sim 2.05$), through an array of 230 SRR cylinders.

B. Negative refraction and superlensing effect

We finally consider a 2D finite phononic crystal surrounded by homogeneous liquid. The crystal consists of 230 rigid cylinders with a “C-shaped” cross section with the same parameters as those of Fig. 2. The crystal has a fourfold (square) symmetry with pitch $d=1$. An acoustic source of wavelength $\lambda_0=3.22d$ is located at a distance $1.4d$ above the top of the crystal. The field map shows the existence of an image of the source, located twice the width of the crystal away. As we can see in Fig. 5, the amplitude of the field is the highest near the thin ligaments Π_e of the SRR. Formula (11) shows that the resonance of the field with the microscopic structure of SRR is responsible for the appearance of negative refraction through negative effective density ρ_{hom} . Finally, the resolution of the image δ is enhanced compared to that obtained using an array of rigid cylinders with a circular or square [31] cross section, as demonstrated in Fig. 6, whereby the full width at half maximum of the image point $\delta \approx \lambda/3$.

Moreover, according to [52], the resolution of a photonic crystal is only limited by its periodicity d ,

$$\frac{1}{2} \frac{d}{1 - \frac{d}{\lambda}} < \delta < d, \quad (26)$$

so that, with the parameters of our simulation, the maximum resolution is equal to $\lambda/3$. This means that in order to maximize the resolution, we ought to decrease the pitch of the crystal (note that from (26) $\lambda > 2d$).

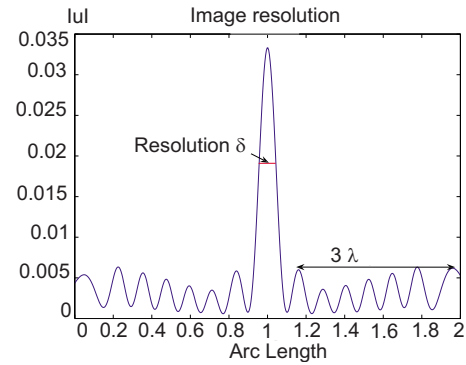


FIG. 6. (Color online) Modulus of the potential ϕ of Fig. 5 along the x_1 direction. The red (gray) line represents the resolution of the image: full width at half maximum of the “image point.”

V. CONCLUSION

We have used the supercell method to derive both the dispersion curves and the field intensities of the LSW modes that can propagate at the surface of a 2D phononic crystal. Calculations were performed for crystals made of cylinders with a split-ring resonator cross section, which are arranged on a square lattice. We demonstrated the existence of surface modes inside the low-frequency band gap of the SRR. And finally, we showed that negative refraction of LSW occurs with a crystal of SRR at the frequency of the surface mode confirming the superlensing effect. Importantly, numerical results are supplied with a homogenization model which demonstrates that negative refraction occurs around the LSW resonances.

The results of this study also hold in the case of antiplane shear waves propagating in an isotropic elastic material structured with an array of cracks shaped as split-ring resonators (Neumann data stand for traction free boundary conditions), see also [53] for a similar design of acoustic metamaterial, as well as in the case of transverse electric waves ($H_{||}$) in an array of infinite conducting SRRs. There is currently some keen interest in acoustic metamaterials, both on theoretical and experimental aspects [54–56]. We hope our results will foster efforts in some of these areas.

ACKNOWLEDGMENTS

A.B.M. and S.G. thank the Engineering and Physical Science Research Council (EPSRC) for funding this research under Grant No. EP/F027125/1.

- [1] V. G. Veselago, *Sov. Phys. Usp.* **10**, 509 (1968).
 [2] J. B. Pendry, *Phys. Rev. Lett.* **85**, 3966 (2000).
 [3] D. R. Smith and N. Kroll, *Phys. Rev. Lett.* **85**, 2933 (2000).
 [4] S. Foteinopoulou, E. N. Economou, and C. M. Soukoulis, *Phys. Rev. Lett.* **90**, 107402 (2003).
 [5] S. A. Ramakrishna, *Rep. Prog. Phys.* **68**, 449 (2005).

- [6] S. Guenneau and S. A. Ramakrishna, *New J. Phys.* **7**, 164 (2005).
 [7] S. Guenneau, B. Gralak, and J. B. Pendry, *Opt. Lett.* **30**, 1204 (2005).
 [8] S. Chakrabarti, S. A. Ramakrishna, and S. Guenneau, *Opt. Express* **14**, 12950 (2006).

- [9] S. A. Ramakrishna, S. Guenneau, S. Enoch, and G. Tayeb, *Phys. Rev. A* **75**, 063830 (2007).
- [10] D. Maystre and S. Enoch, *J. Opt. Soc. Am. A* **21**, 122 (2004).
- [11] B. Gralak, S. Enoch, and G. Tayeb, *J. Opt. Soc. Am. A* **17**, 1012 (2000).
- [12] J. B. Pendry and S. A. Ramakrishna, *J. Phys.: Condens. Matter* **15**, 6345 (2003).
- [13] T. Decoopman, G. Tayeb, S. Enoch, D. Maystre, and B. Gralak, *Phys. Rev. Lett.* **97**, 073905 (2006).
- [14] J. B. Pendry, D. Schurig, and D. R. Smith, *Science* **312**, 1780 (2006).
- [15] D. Schurig, J. J. Mock, B. J. Justice, S. A. Cummer, J. B. Pendry, A. F. Starr, and D. R. Smith, *Science* **314**, 977 (2006).
- [16] G. W. Milton and N.-A. P. Nicorovici, *Proc. R. Soc. London, Ser. A* **462**, 3027 (2006).
- [17] F. Zolla, S. Guenneau, A. Nicolet, and J. B. Pendry, *Opt. Lett.* **32**, 1069 (2007).
- [18] N. A. Nicorovici, R. C. McPhedran, and G. W. Milton, *Phys. Rev. B* **49**, 8479 (1994).
- [19] M. Farhat, S. Guenneau, A. B. Movchan, and S. Enoch, *Opt. Express* **16**, 5656 (2008).
- [20] V. V. Jikhov, S. M. Kozlov, and O. A. Oleinik, *Homogenization of Differential Operators and Integral Functionals* (Springer Verlag, New York, 1994).
- [21] M. Codegone and A. Negro, *Appl. Anal.* **18**, 159 (1984).
- [22] S. Guenneau and F. Zolla, *J. Electromagn. Waves Appl.* **14**, 529 (2000); *Prog. Electromagn. Res.* **27**, 91 (2000).
- [23] G. Kristensson and N. Wellander, *SIAM J. Appl. Math.* **64**, 170 (2003).
- [24] C. G. Poulton, S. Guenneau, and A. B. Movchan, *Phys. Rev. B* **69**, 195112 (2004).
- [25] D. R. Smith and J. B. Pendry, *J. Opt. Soc. Am. B* **23**, 391 (2006).
- [26] S. Guenneau, F. Zolla, and A. Nicolet, *Waves Random Complex Media* **17**, 653 (2007).
- [27] S. Guenneau and F. Zolla, *Physica B* **394**, 145 (2007).
- [28] X. Hu, Y. Shen, X. Liu, R. Fu, and J. Zi, *Phys. Rev. E* **69**, 030201(R) (2004).
- [29] P. McIver, *J. Fluid Mech.* **424**, 101 (2000).
- [30] M. Torres, J. P. Abrados, F. R. Montero de Espinosa, D. Garcia-Pablos, and J. Fayos, *Phys. Rev. E* **63**, 011204 (2000).
- [31] M. Farhat, S. Guenneau, S. Enoch, G. Tayeb, A. B. Movchan, and N. V. Movchan, *Phys. Rev. E* **77**, 046308 (2008).
- [32] M. Farhat, S. Enoch, S. Guenneau, and A. B. Movchan, *Phys. Rev. Lett.* **101**, 134501 (2008).
- [33] J. B. Pendry, A. J. Holden, D. J. Robbins, and W. J. Stewart, *IEEE Trans. Microwave Theory Tech.* **47**, 2075 (1999).
- [34] A. B. Movchan and S. Guenneau, *Phys. Rev. B* **70**, 125116 (2004).
- [35] S. Guenneau, A. B. Movchan, and N. V. Movchan, *Physica B* **394**, 141 (2007).
- [36] S. Enoch, E. Popov, and N. Bonod, *Phys. Rev. B* **72**, 155101 (2005).
- [37] J. Merle Elson and K. Halterman, *Opt. Express* **12**, 4855 (2004).
- [38] R. D. Meade, K. D. Brommer, A. M. Rappe, and J. D. Joannopoulos, *Phys. Rev. B* **44**, 10961 (1991).
- [39] V. V. Zhikov, *Sb. Math.* **191**, 973 (2000).
- [40] G. Bouchitté and D. Felbacq, *C. R. Math.* **339**, 377 (2004).
- [41] A. Avila, G. Griso, and B. Miara, *C. R. Math.* **340**, 933 (2005).
- [42] K. D. Cherednichenko, V. P. Smyshlyaev, and V. V. Zhikov, *Proc. - R. Soc. Edinburgh, Sect. A: Math.* **136**, 87 (2006).
- [43] R. V. Kohn and S. Shipman, *Multiscale Model. Simul.* **7**, 62 (2008).
- [44] S. O'Brien and J. B. Pendry, *J. Phys.: Condens. Matter* **14**, 6383 (2002).
- [45] A. B. Movchan and N. V. Movchan, *Mathematical Modelling of Solids with Non-regular Boundaries* (CRC Press, Boca Raton, FL, 1995).
- [46] V. Kozlov, V. Maz'ya, and A. B. Movchan, *Fields in Multistructures. Asymptotic Analysis* (Oxford University Press, Oxford, 1999).
- [47] V. G. Maz'ya and M. Hanler, *Math. Nachr.* **162**, 261 (1993).
- [48] This liquid is HFE-7100 (nonafluorobutyl methyl ether) a solvent with a viscosity $\nu=0.61 \times 10^{-2}$ cm²/s, a surface tension $\sigma=13.6$ N/cm, and a density $\rho=1.529$ g/ml.
- [49] N. Kuznetsov, V. Maz'ya, and B. Vainberg, *Linear Water Waves: A Mathematical Approach* (Cambridge University Press, Cambridge, England, 2002).
- [50] A. Nicolet, S. Guenneau, C. Geuzaine, and F. Zolla, *J. Comput. Appl. Math.* **168**, 321 (2004).
- [51] J. B. Pendry, L. Martin-Moreno, and F. J. Garcia-Vidal, *Science* **305**, 847 (2004).
- [52] George V. Eleftheriades and Keith G. Balmain, *Negative-Refraction Metamaterials: Fundamental Principles and Applications* (Wiley, New York, 2005), Chap. 7.
- [53] S. Guenneau, A. B. Movchan, G. Petursson, and S. A. Ramakrishna, *New J. Phys.* **9**, 399 (2007).
- [54] Y. Ding, Z. Liu, C. Qiu, and J. Shi, *Phys. Rev. Lett.* **99**, 093904 (2007).
- [55] A. Sukhovich, L. Jing, and J. H. Page, *Phys. Rev. B* **77**, 014301 (2008).
- [56] S. Zhang, L. Yin, and N. Fang, *Phys. Rev. Lett.* **102**, 194301 (2009).